NMR, PDF and RMC study of the positive electrode material $Li(Ni_{0.5}Mn_{0.5})O_2$ synthesized by ion-exchange methods†‡

Julien Bréger,[a] Kisuk Kang,[b] Jordi Cabana,[a] Gerbrand Ceder[b] and Clare P. Grey*[a]

Received 22nd February 2007, Accepted 2nd May 2007
First published as an Advance Article on the web 18th May 2007
DOI: 10.1039/b702745a

The local environment and short-range ordering of $Li(Ni_{0.5}Mn_{0.5})O_2$, a potential Li-ion battery positive electrode material obtained *via* an ion-exchange route from $Na(Ni_{0.5}Mn_{0.5})O_2$, were investigated by using a combination of ^{6}Li Magic Angle Spinning (MAS) NMR spectroscopy and neutron Pair Distribution Function (PDF) analysis, associated with Reverse Monte Carlo (RMC) calculations. ^{6}Li MAS NMR experiments on $Li(Ni_{0.5}Mn_{0.5})O_2$ showed that there are almost no Li ions in the transition metal layers. Neutron diffraction data for the precursor $Na(Ni_{0.5}Mn_{0.5})O_2$ indicated that there is no Na/Ni disorder and that the material is perfectly layered. Neutron PDF analysis of $Li(Ni_{0.5}Mn_{0.5})O_2$ and $Na(Ni_{0.5}Mn_{0.5})O_2$ revealed differences in the local transition metal arrangements between those present in the ion-exchanged material and its precursor, and those found in the cathode material synthesized directly from hydroxide starting materials. Large clusters of 3456 atoms were built to investigate cation ordering. Reverse Monte Carlo results, for both the Na and Li-containing compounds, showed a non-random distribution of Ni and Mn cations in the transition metal layers: in the first coordination shell, Ni atoms are on average close to more Mn ions than predicted based on a random distribution of these ions in the transition metal layers. Analysis of the number of Ni/Ni, Mn/Mn and Ni/Mn pairs in the second coordination shell revealed that the Ni and Mn cations show a clear preference for ordering in zigzags rather than in chains.

Introduction

Much recent effort has been made to develop new, alternative intercalation compounds to $LiCoO_2$, the material that is used as a positive electrode in rechargeable Li batteries in many commercial applications including cell phones and laptops. Among these compounds, $Li(Ni_{0.5}Mn_{0.5})O_2$ is particularly attractive due to its lower cost and toxicity, and its high theoretical capacity (280 mAh g^{-1}). It has therefore been widely investigated over the past few years.[1–3] $Li(Ni_{0.5}Mn_{0.5})O_2$ is isostructural with α-$NaFeO_2$[4] (space group $R\bar{3}m$) and consists of a layered structure. In the material prepared by using a mixed nickel/manganese hydroxide, solid-state route, which will be referred to as SS-$Li(Ni_{0.5}Mn_{0.5})O_2$, a considerable amount ($\sim$10%) of Li and Ni is exchanged between the Li and the transition metal (TM) layers.[5–7] In our previous structural work on this system,[8] we applied Pair Distribution Function (PDF) analysis, in combination with the Reverse Monte Carlo (RMC) technique and ^{6}Li Magic Angle Spinning (MAS) Nuclear Magnetic Resonance (NMR) spectroscopy, to investigate the nature of cation ordering in the TM layers. The results provided clear evidence for a non-random cation distribution: fewer Ni/Ni and more Ni/Mn pairs were observed in the first cation coordination shell than predicted based on a random model. PDF and NMR results were consistent with an ordering scheme intermediate between the ideal structures proposed so far [(a) the ''honey-comb'' structure, proposed based on TEM data for $Li(Ni_{0.5}Mn_{0.5})O_2$[9] and NMR[10] and diffraction data[11] for the Li-rich materials, and (b) the ''flower'' structure predicted from first principle calculations by Van der Ven and Ceder[12]].

Recently, it was shown that a more layered version of $Li(Ni_{0.5}Mn_{0.5})O_2$, obtained *via* an ion-exchange (IE) process using $Na(Ni_{0.5}Mn_{0.5})O_2$ as a precursor [IE-$Li(Ni_{0.5}Mn_{0.5})O_2$], can rival the rate capability of the Co-substituted materials.[13] This excellent rate performance was ascribed to a reduction in the Li/Ni exchange, as seen by Li NMR and XRD.[13] The stability of various cation ordering schemes has been investigated in previous theoretical investigations of cation ordering in $Li(Ni_{0.5}Mn_{0.5})O_2$, for materials that do not contain Li in the TM layers. Islam *et al.* first showed that different cation ordering schemes were associated with large energy differences, the results indicating that the configurational entropy terms would likely be insufficient to generate random distributions of cations in these materials.[14] They observed that structures containing Ni and Mn ions ordered in chains (Fig. 1, left), were energetically favored over those with alternating 100% Ni and 100% Mn layers; furthermore, large energy differences were observed depending on how the chains were stacked in the third dimension, the lowest energy chain structure being obtained for a symmetric stacking of the chains.[14] Our later theoretical study suggested that a Ni/Mn

[a]*Dept of Chemistry, SUNY Stony Brook, Stony Brook, NY 11790, USA. E-mail: cgrey@notes.cc.sunysb.edu; Fax: +1 631 632 5731*
[b]*Dept of Materials Science and Engineering, Massachusetts Institute of Technology, Cambridge, MA 02139, USA*

† This paper is part of a *Journal of Materials Chemistry* theme issue on New Energy Materials. Guest editor: M. Saiful Islam.

‡ Electronic supplementary information (ESI) available: Rietveld refinements, reverse Monte Carlo results and ^{23}Na MAS NMR spectra. See DOI: 10.1039/b702745a

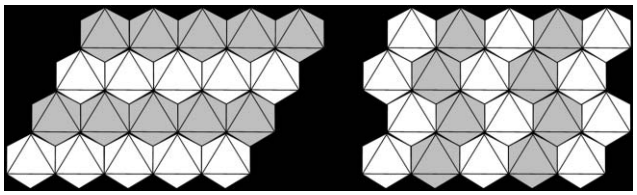

Fig. 1 Different in-plane (*ab* plane) orderings of Ni (dark octahedra) and Mn (white octahedra) in $Li(Ni_{0.5}Mn_{0.5})O_2$, for which no Li are present in the Ni/Mn layers: left, ''chain'' and right, ''zigzag'' arrangements.

''zigzag'' arrangement (Fig. 1, right) is lower in energy than the ''chain'' structure.[10] Both these structures have identical transition metal coordination environments in the first cation coordination shell but differ in the second cation coordination shell. The different stacking schemes also generate different local environments for Li in both the first and second cation coordination shells, which will also vary depending on how the layers are stacked in the third dimension.

The nature of cation ordering can strongly affect the electrochemical performance and stability of a material. Thus, the aim of the work presented in this paper was to experimentally investigate the Ni/Mn cation ordering in the TM layers of IE-$Li(Ni_{0.5}Mn_{0.5})O_2$ and the precursor material $Na(Ni_{0.5}Mn_{0.5})O_2$, by using neutron PDF analysis associated with RMC calculations and NMR spectroscopy.

Experimental

Materials preparation

$Na(Ni_{0.5}Mn_{0.5})O_2$ was prepared by a solid-state reaction following two routes. The first route used Na_2CO_3 (>99.5%, Aldrich), $Ni(OH)_2$ (99.3%, J.T. Baker) and Mn_2O_3 (>99.9%, Aldrich) as reagents. The appropriate amounts of these starting materials were wet ball-milled for 1 d. After drying, this mixture was ground using a mortar, and pressed into a pellet. The pellet was heated at 900 °C for 24 h in air. The pellet was quenched to room temperature by using a copper plate. This sample was labeled $Na(Ni_{0.5}Mn_{0.5})O_2$-I. The second route [$Na(Ni_{0.5}Mn_{0.5})O_2$-II] involved the use of Na_2CO_3 and $(Ni_{0.5}Mn_{0.5})(OH)_2$. The mixed hydroxide was prepared by slowly dripping 50 ml of an aqueous solution of stoichiometric amounts of $Mn(NO_3)_2{\cdot}4H_2O$ (Fluka, >97%) and $Ni(NO_3)_2{\cdot}6H_2O$ (Aldrich, 99.999%) into 400 ml of a stirred solution of $LiOH{\cdot}H_2O$ (Sigma-Aldrich, >98%). The resulting brown precipitate was dried at 180 °C for 14 h, and then mixed with Na_2CO_3 in stoichiometric proportions. The mixture was then heated in air at 800 °C for a total of 30 h, with intermediate grinding after 15 h, and quenched using liquid nitrogen. The percentages of Na, Ni and Mn obtained by ICP elemental analysis of this sample (Galbraith Laboratories Inc. USA) were 20.4, 26.4, and 24.7 wt%, respectively, consistent with Na : Ni : Mn stoichiometry ratios of 1 : 0.5 : 0.5. Both samples were transferred to an Ar-filled glove box immediately after quenching to avoid any reaction with moisture.

To obtain IE-$Li(Ni_{0.5}Mn_{0.5})O_2$ by ion-exchange, $Na(Ni_{0.5}Mn_{0.5})O_2$-I was mixed with the eutectic composition of $LiNO_3$ (99.98%, Alfa Aesar) and LiCl (99%, Mallinckrodt) containing a 10 times Li molar excess. The mixture was heated at 280 °C for 5 h in air. After ion-exchange, the mixture was rinsed with distilled water and ethanol several times, and filtered to recover the powder. The whole ion-exchange process was repeated once more in order to have complete ion-exchange. Finally, the Li-containing dark brown powder was dried in air for a day in an oven.

Neutron diffraction

Neutron diffraction experiments were performed on the General Materials Diffractometer (GEM) instrument at ISIS (Didcot, UK) for $Na(Ni_{0.5}Mn_{0.5})O_2$-I and on the General Purpose Powder Diffractometer (GPPD) at the Intense Pulsed Neutron Source (IPNS, Argonne National Laboratory, USA) for -II and $Li(Ni_{0.5}Mn_{0.5})O_2$. The samples (from 300 mg to 1 g) were packed into 5 mm (inner diameter) thin-walled vanadium cans. The exposure time for each sample was from 12 to 15 h. The data were corrected for instrument background, sample and background absorption and multiple scattering. Data up to Q_{max} = 30 $Å^{-1}$ for $Na(Ni_{0.5}Mn_{0.5})O_2$ and Q_{max} = 18 $Å^{-1}$ for $Li(Ni_{0.5}Mn_{0.5})O_2$ were used in the Fourier transform. The PDF data obtained from these neutron experiments were processed using the Gudrun software[15] for $Na(Ni_{0.5}Mn_{0.5})O_2$-I and PDFgetN[16] for $Na(Ni_{0.5}Mn_{0.5})O_2$-II and IE-$Li(Ni_{0.5}Mn_{0.5})O_2$.

MAS NMR spectroscopy

^6Li MAS NMR spectroscopy was performed on the IE-$Li(Ni_{0.5}Mn_{0.5})O_2$ sample, with a double-resonance 2 mm probe, built by Samoson and coworkers,[17] on a CMX-200 spectrometer using a magnetic field of 4.7 T. The spectrum was collected at an operating frequency of 29.46 MHz. A spinning frequency of 40 kHz and a rotor-synchronized spin-echo sequence (90°–τ–180°–τ–acq) were used to acquire the spectra. $\pi/2$ pulses of 2.8 μs were used, with a delay time of 0.2 s. The spectrum was referenced to 1 M ^6LiCl solution, at 0 ppm.

Results and analysis for $Na(Ni_{0.5}Mn_{0.5})O_2$

Neutron diffraction

Fig. 2 shows the neutron diffraction pattern of $Na(Ni_{0.5}Mn_{0.5})O_2$-I, derived *via* the carbonate route. Rietveld[18] refinements of the structure were performed with these data using GSAS-EXPGUI.[19] A good agreement was seen between the experimental data and the patterns calculated with the $LiCoO_2$ structural model (space group $R\bar{3}m$). The corresponding structural parameters obtained with this model are listed in Table 1. Allowing Na/Ni exchange between the Ni/Mn and Na layers of $Na(Ni_{0.5}Mn_{0.5})O_2$, yielded a negative occupancy of Ni in the Na layer, indicating that the Na/Ni exchange is negligible, as expected based on the large difference in ionic radii of these two cations.[20] Close examination of the diffraction patterns revealed weaker peaks, which could not be indexed with the $R\bar{3}m$ space group, due to NiO present as an impurity phase. Considerable effort, including changing the temperature and length of the heat treatments, was made to remove this impurity from our samples, but it proved to be extremely difficult to eliminate it completely.

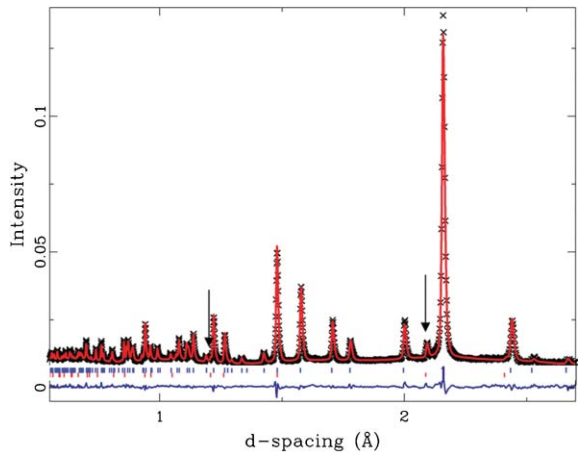

Fig. 2 Rietveld refinement using the neutron diffraction pattern (bank 3—from 25° and 45°—of the GEM detector) of $Na(Ni_{0.5}Mn_{0.5})O_2$-I. The crosses and the solid red line represent the experimental and the calculated patterns, respectively. The difference between the two patterns is shown in blue below. The arrows and red tickmarks show the reflections coming from NiO impurities. The structural parameters are given in Table 1.

Table 1 Rietveld refinement results for the $Na(Ni_{0.5}Mn_{0.5})O_2$-I neutron diffraction pattern. A simultaneous refinement with the same parameters, with three different histograms, corresponding to banks 3, 4, and 5 of the GEM detector, were performed

	$Na(Ni_{0.5}Mn_{0.5})O_2$	NiO impurity[21]
Space group	$R\bar{3}m$	$Fm\bar{3}m$
a/Å	2.95574(4)	4.1825(2)
c/Å	16.0045(5)	—
V/Å^3	121.089(3)	73.16(1)
z/O	0.23184(4)	—
Na occupancy	0.879(2)	—
Ni occupancy	0.493(1)	—
Mn occupancy	0.501(3)	—
$100U_{iso}$/Å^2		
Na (3a)	1.69(5)	Ni (0,0,0): 0.239(2)
Ni, Mn (3b)	1.56(3)	O (1/2,1/2,1/2):0.25
O (6c)	1.41(3)	
Weight fraction	98.9%	1.1%
Bank 3 (25–45°)	R_{wp} = 2.90%	
Bank 4 (50–75°)	R_{wp} = 2.37%	
Bank 5 (79–104°)	R_{wp} = 2.71%	

Whether this is due to incomplete reaction (*i.e.*, the yield was not 100%) or to the possible presence of Na vacancies is not clear at this point. To determine the amount of NiO present in the sample, a two-phase refinement was performed and weight fractions of 1.1% of NiO and 98.9% of $Na(Ni_{0.5}Mn_{0.5})O_2$ were found.

The cell parameters were similar to those obtained previously from laboratory X-ray diffraction[13] and the c-parameter is noticeably larger than the one observed for SS-^{7}Li$(Ni_{0.5}Mn_{0.5})O_2$ [c = 14.262(1) Å],[8] due to the larger ionic radius of Na^+ in comparison to that of Li^+. The Na occupancy was allowed to vary in the refinement and was determined to be 0.879(2). This value is only slightly lower than the one obtained from previous XRD refinements (0.925).[13] The Ni and Mn occupancies were also refined and a Ni : Mn ratio of 49.3 : 50.1 was obtained, which is very close to the theoretical value of 50 : 50.

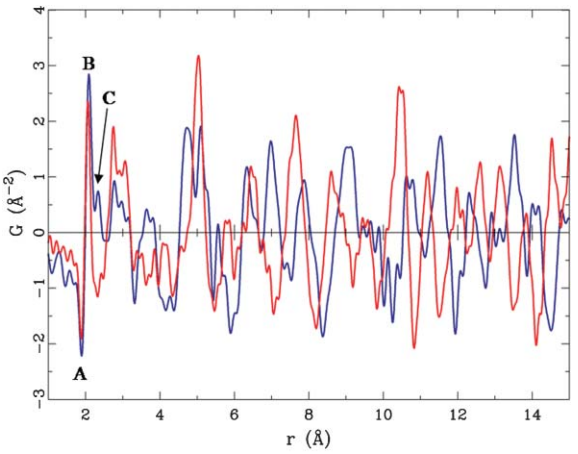

Fig. 3 Pair distribution functions [PDF, $G(r)$] for SS-^{7}Li$(Ni_{0.5}Mn_{0.5})O_2$ (red) and $Na(Ni_{0.5}Mn_{0.5})O_2$-I (blue). The PDF intensities were normalized using the first correlation (Mn^{4+}–O). The peaks assignments are: A: Mn–O distances, B: Ni–O and Li–O distances and C: Na–O distances.

A two-phase Rietveld refinement was similarly performed using the data acquired for $Na(Ni_{0.5}Mn_{0.5})O_2$-II. The weight fraction of NiO impurity was found to be slightly larger (~2%). A Ni/Mn ratio close to 1.0, and cell parameter values of a = 2.9579 Å and c = 15.942 Å, with a total R_{wp} equal to 4.6% were obtained (see ESI, Table S1‡). A larger Na occupancy (0.98) was found. At this point, it is not clear whether this is significant, since the difference in Na occupancies between the two sodium phases is within the error sometimes found for occupancies obtained from Rietveld refinements of these types of materials.

PDF analysis

The neutron Pair Distribution Function (PDF) was calculated from the neutron diffraction data for $Na(Ni_{0.5}Mn_{0.5})O_2$-I (Fig. 3), and compared to PDF data obtained previously for SS-^{7}Li$(Ni_{0.5}Mn_{0.5})O_2$.[8] Note that the PDF calculation uses all the scattering data and is not dependent on the model used to describe the diffraction data. The intensities were normalized (to allow comparison between samples) by using the scale factors obtained in the Rietveld refinements and the experiment time. As shown before,[8] the first correlation distance (A in Fig. 3) corresponds to the Mn^{4+}–O pairs. The intensity of this peak is negative, since the coherent scattering length of Mn atoms (see Table 2) is negative [b(Mn) = −3.73 fm]. For the SS-^{7}Li$(Ni_{0.5}Mn_{0.5})O_2$, the second peak at 2.09 Å (B) was ascribed to the Ni/Li–O bonds.[8] However, since the Li^+–O and Ni^{2+}–O distances are so close, two separate peaks could not be resolved in this PDF data. Peak B is more intense in $Na(Ni_{0.5}Mn_{0.5})O_2$ due to the absence of the Li–O correlations, which give rise to peaks with negative intensities due to the

Table 2 Coherent neutron scattering lengths b_i (fm) of the different isotopes[22]

^{7}Li	Li	Na	Ni	Mn	O
−2.22	−1.90	3.63	10.3	−3.73	5.80

negative scattering length of ^{7}Li. For the $Na(Ni_{0.5}Mn_{0.5})O_2$ compound, a third positive peak (C) is also seen at around 2.34 Å, which can assigned to Na^{+}–O correlations, since *b*(Na) is positive. The PDF data clearly demonstrates that the M–O distances in the TM layers are unchanged between the Li and Na forms, the increase in the interlayer space arising from the larger average alkali M–O distance in $Na(Ni_{0.5}Mn_{0.5})O_2$.

Reverse Monte Carlo calculations

The Reverse Monte Carlo (RMC) technique[23,24] was used in order to explore possible ordering of the Ni/Mn atoms in the $Na(Ni_{0.5}Mn_{0.5})O_2$ precusor, using a similar approach to that used for SS-^{7}Li$(Ni_{0.5}Mn_{0.5})O_2$.[8] The cell parameters determined from Rietveld refinement of the neutron diffraction data were used in the RMC calculations. A cluster comprising 12 × 12 × 2 (*a* × *a* × *c*) unit cells (3456 atoms) was built, containing 0% Na/Ni site exchange and 0.87 Na, as seen from the neutron Rietveld refinement of the same sample, and with Ni and Mn atoms randomly distributed in the TM layers.

The NiO impurity was not included in the RMC calculations, due to the low NiO weight fraction. RMC calculations were performed with the DISCUS program.[25] During the calculations, Ni and Mn atoms were swapped randomly and all the atoms were allowed to relax in the *ab* plane. If a generated move improved the fit, the move was accepted. The final calculated PDF is shown in Fig. 4(b) and, even though the fit is not perfect, a clear improvement of the fit of the experimental data over that calculated from the ideal $LiCoO_2$ model (where a random distribution of Ni and Mn atoms in the TM layers is assumed) was obtained [Fig. 4(a)] and most of the major features appear to be captured.

The values for the Ni/Ni, Ni/Mn and Mn/Mn pairs are reported in Table 3. These clearly show a non-random distribution of Ni and Mn cations in the TM layers, with Ni closer to Mn in the first coordination shell and to Ni in the second coordination shell.

RMC calculations were also performed for $Na(Ni_{0.5}Mn_{0.5})O_2$-II by using the same procedure. The results are qualitatively similar, but a significantly better fit was obtained than for sample II [Fig. 4(c)]. The improved fit may be due to the slight difference in sample composition or the fact that the data were collected on different diffractometers (although the data were acquired out to the same *Q* value). Again, the RMC results for sample II are consistent with a non-random distribution of transition metal ions (Table 3), the data showing even stronger tendencies for Ni/Mn pair formation and Ni–Ni and Mn–Mn avoidance.

The effect of cell size on the fit to the PDF data for $Na(Ni_{0.5}Mn_{0.5})O_2$-II was explored by constructing a smaller cluster now comprising only 10 × 10 × 2 unit cells; the quality of the fit was essentially identical (χ^2 = 0.66) to the one obtained with the larger cell (χ^2 = 0.6), and similar cation distributions were obtained. The data were also examined for any evidence for correlations between the stacking of the transition metal layers. The concentrations of each type of nearest M/M pair in two different TM layers (separated by approx. 5.6 Å) were determined and the numbers of Ni/Ni, Ni/Mn, and Mn/Mn pairs were consistent with those predicted assuming random stacking in the third dimension (the *c*-direction).

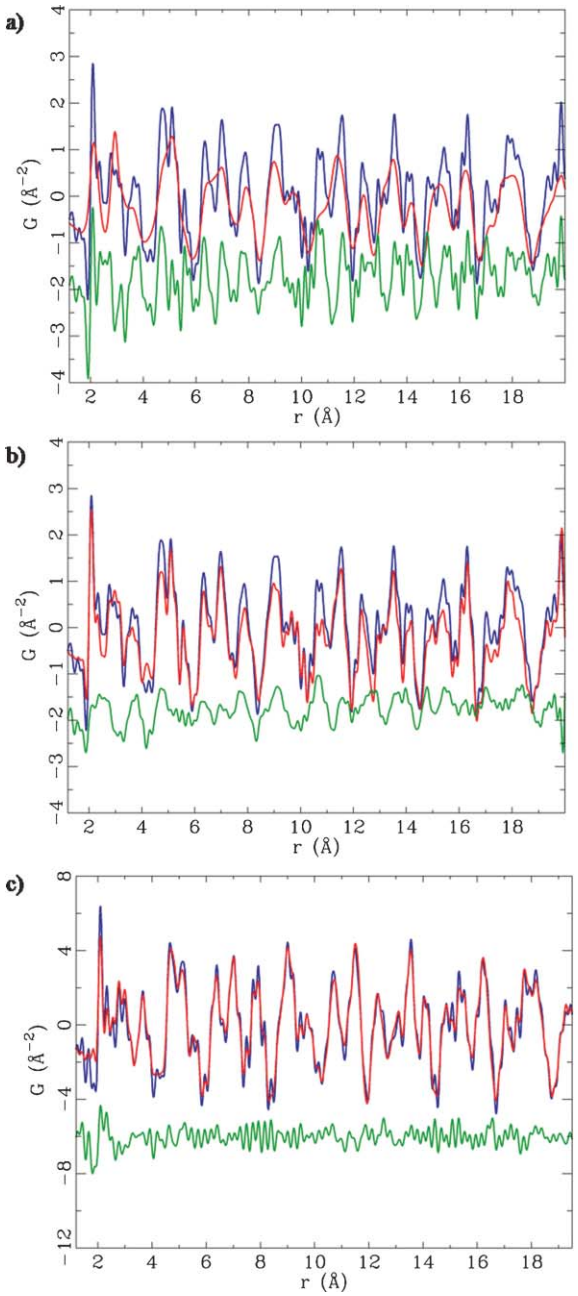

Fig. 4 Reverse Monte Carlo (RMC) results for the $Na(Ni_{0.5}Mn_{0.5})O_2$ precursors: (a) fit before the RMC calculations for $Na(Ni_{0.5}Mn_{0.5})O_2$-I with the initial random cluster model and after for (b) -I and (c) -II. The blue line represents the experimental data and the red line the calculated PDFs. The difference between the calculated and experimental PDFs is shown in green.

Results and analysis for IE-Li$(Ni_{0.5}Mn_{0.5})O_2$

NMR

Fig. 5(a) shows the ^{6}Li MAS NMR spectrum of IE-Li$(Ni_{0.5}Mn_{0.5})O_2$ obtained with a spinning frequency of 40 kHz.[10] The spectrum is consistent with the work of

Table 3 Number of Ni/Mn pairs in the transition metal layers (*ab* plane) of $Na(Ni_{0.5}Mn_{0.5})O_2$ and correlations for the occupancies before (sample I) and after the RMC calculations (samples I and II), for the 12 × 12 × 2 cluster size and for the first and second coordination shells. The initial starting model for sample II is given in Table S3

	$R\bar{3}m$ Space group 12 × 12 × 2 cluster			
	1st Coordination shell		2nd Coordination shell	
	Before (random: I)	After: I; II	Before (random: I)	After: I; II
Ni/Ni pairs (%)	24.2	22.5; 19.8	24.5	27.1; 26.0
Ni/Mn pairs (%)	50.9	54.2; 56.5	50.2	45.1; 44.1
Mn/Mn pairs (%)	24.9	23.3; 23.7	25.3	27.8; 29.9
Total (%)	100	100	100	100
Correlation c_{NiMn}[a]	−0.02	−0.13; −0.16	0.00	+0.06; 0.10

[a] The correlation coefficient c_{ij} between a pair of sites i and j is given by the statistical definition[26] of the correlation: $c_{ij} = (P_{ij} - \theta^2)/[\theta(1 - \theta)]$, where P_{ij} is the probability that both sites i and j are occupied by the same atom type and θ is its overall occupancy. Negative values of c_{ij} indicate that the sites i and j tend to be occupied by different atom types.

Yoon *et al.*[5] and consists of two groups of resonances, one at around 670 ppm corresponding to Li in the Li layers and the other around 1450 ppm corresponding to Li in the TM layers. The comparison of this spectrum to SS-$Li(Ni_{0.5}Mn_{0.5})O_2$ [Fig. 5(b)][8] clearly shows that the amount of Li in transition metal layers has significantly decreased. A value for the concentration of Li in transition metal layers of 0.5% of the total Li content [compared to 9 ± 2% for the SS-$Li(Ni_{0.5}Mn_{0.5})O_2$ compound][8] was determined by integration of the intensities of the different signals. The NMR data clearly indicate that ion-exchange of $Na(Ni_{0.5}Mn_{0.5})O_2$-I *via* the molten salt route does not lead to the incorporation of Li into the transition metal layers of $Li(Ni_{0.5}Mn_{0.5})O_2$.[13]

The ^{23}Na MAS NMR spectra of $Na(Ni_{0.5}Mn_{0.5})O_2$-I and -II contain a single very broad resonance, which spreads over 500–3500 ppm (*ca.* 150 kHz, see ESI, Fig. S5). This large width indicates that the isotropic resonance(s) resulting from these compounds are so broad that they overlap with their corresponding sidebands and sidebands from other isotropic resonances even at the high spinning speeds that can be reached in our experimental setup (38–40 kHz). This makes it very difficult to extract detailed information concerning the nature and number of local environments present in the sample. Qualitatively, however, these spectra are comparable to the ^6Li MAS NMR spectrum of IE-$Li(Ni_{0.5}Mn_{0.5})O_2$, in that a very broad resonance dominates both sets of spectra.

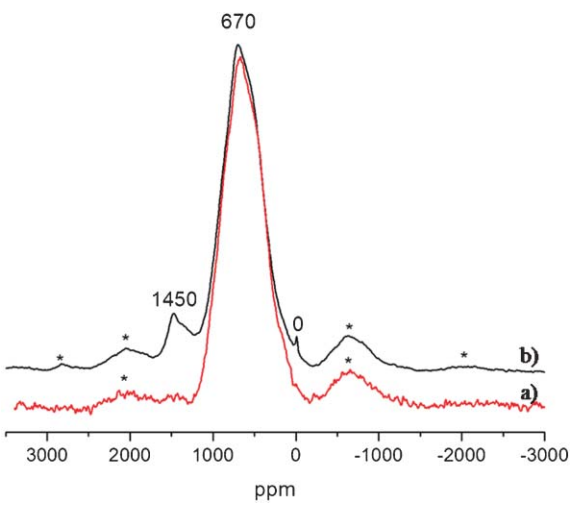

Fig. 5 ^6Li MAS NMR spectra of (a) IE-$Li(Ni_{0.5}Mn_{0.5})O_2$ and (b) SS-$Li(Ni_{0.5}Mn_{0.5})O_2$. The resonance at 0 ppm arises from diamagnetic impurities (Li_2O for instance). The major isotropic resonances and spinning sidebands are marked with their shifts and asterisks, respectively.

Neutron diffraction

Rietveld[18] refinement of the structure of IE-$Li(Ni_{0.5}Mn_{0.5})O_2$ was attempted by using the neutron diffraction data. Unfortunately, the refinement was not sucessful due to the large background present in the data, arising from the strong absorption of the ^6Li nuclei (the sample was not enriched in ^7Li) and possibly some protons incorporated during the ion-exchange process. Even though the Li occupancy in the layers could not be refined, cell parameters could be obtained: c = 14.343(1) Å and a = 2.8953(1) Å, with a R_{wp} of 5.29%. These values were in excellent agreement with values obtained from previous XRD refinements: c = 14.3437(8) Å and a = 2.8924(1) Å, R_{wp} = 8.74%.[10] It should be noted that there is a noticeable increase in the c-parameter from 14.262 Å in SS-$^7Li(Ni_{0.5}Mn_{0.5})O_2$[8] to 14.343 Å in IE-$Li(Ni_{0.5}Mn_{0.5})O_2$, which is ascribed to the reduced concentration of Ni present in the Li layers in the IE sample (approx. 4.3%, based on the XRD refinements).[13]

PDF analysis

The neutron Pair Distribution Function (PDF) was calculated from the neutron diffraction data for IE-$Li(Ni_{0.5}Mn_{0.5})O_2$ (Fig. 6), and compared to the one obtained for SS-$^7Li(Ni_{0.5}Mn_{0.5})O_2$.[8] Since the scale factor could not be refined for the ion-exchanged sample, to allow comparison between samples, the intensities were normalized by using the first intense peak (at 1.89 Å) in the $G(r)$ plot, which corresponds to the Mn^{4+}–O bond distance. The second peak at 2.09 Å was ascribed to the Ni/Li–O bonds. At least three peaks are seen for both compounds at around 3 Å, due to M–M, Li–M, and O–O closest contacts. The intensities of these three peaks differ between the IE and the SS sample indicative of different cation distributions.

Reverse Monte Carlo calculations

The cell parameters determined from Rietveld refinement of the neutron data were used in the RMC calculations for

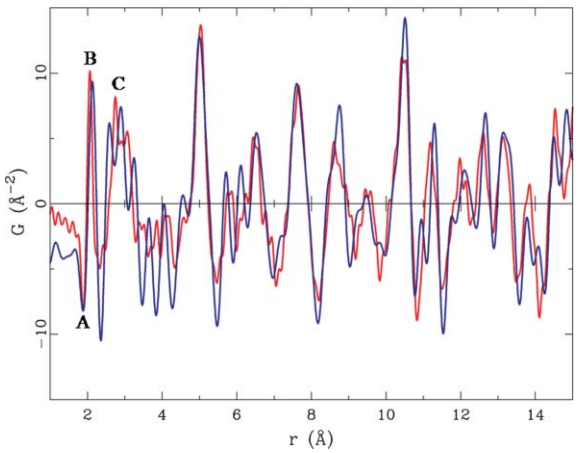

Fig. 6 Pair distribution functions [PDF, $G(r)$] of SS-^{7}Li($Ni_{0.5}Mn_{0.5}$)O_2 (red) and IE-Li($Ni_{0.5}Mn_{0.5}$)O_2 (blue) materials. The PDF intensities were normalized by using the first correlation (Mn^{4+}–O). The peaks assignments are: A: Mn–O distances, B: Ni–O and Li–O distances and C: M–M (where M = Ni, Mn and Li) and O–O closest contacts.

IE-Li($Ni_{0.5}Mn_{0.5}$)O_2. A cluster comprising 12 × 12 × 2 (a × a × c) unit cells (3456 atoms), was built, containing no Li/Ni site exchange and with Ni and Mn atoms randomly distributed in the TM layers. Again, a significant improvement to the fit is obtained after the RMC calculations [Fig. 7(b)].

The values for the number of Ni/Ni, Ni/Mn and Mn/Mn pairs are reported in Table 4. As observed for Na($Ni_{0.5}Mn_{0.5}$)O_2, they clearly show a non-random distribution of Ni and Mn cations in the TM layers, with Ni closer to Mn in the first coordination shell and to Ni in the second coordination shell. Three RMC calculations were performed on the IE-Li($Ni_{0.5}Mn_{0.5}$)O_2 sample using different initial random structures and the results were very similar. A similar increase in the numbers of Ni/Mn pairs and decrease in Ni/Ni and Mn/Mn pairs in the first coordination shell, over the numbers found in the random structure, were observed.

Discussion and comparison with ordered models

PDF analysis, associated with RMC calculations, shows a non-random distribution of cations in the Ni/Mn layers in both IE-Li($Ni_{0.5}Mn_{0.5}$)O_2 and its precursor, Na($Ni_{0.5}Mn_{0.5}$)O_2. Both sets of compounds show the same tendency for Ni/Mn ordering: Ni is surrounded by more Mn in the first coordination shell and by more Ni in the second coordination shell. For example, in IE-Li($Ni_{0.5}Mn_{0.5}$)O_2, the Ni atoms are, on average, surrounded by 2.39 Ni and 3.61 Mn ions in the first coordination shell, and by 4.16 Ni and 1.84 Mn ions in the second coordination shell (Table 4). The apparent degree of ordering increases from Na($Ni_{0.5}Mn_{0.5}$)O_2-I to -II to IE-Li($Ni_{0.5}Mn_{0.5}$)O_2, the ordering appearing to be more pronounced for the IE sample than for the precursor from which it is derived, Na($Ni_{0.5}Mn_{0.5}$)O_2-I. However, it seems somewhat unlikely that the Ni/Mn cation ordering increases during the low temperature ion-exchange process and the apparent weaker ordering for -I may simply be a consequence of (i) the poorer fit to the PDF data for this sample, (ii) the lower quality data for the lithiated material, and/or (iii) to errors arising from the fact that the NiO impurities were not included in the RMC calculations. Incorrect modelling of the Na distributions may also introduce errors. The variations in

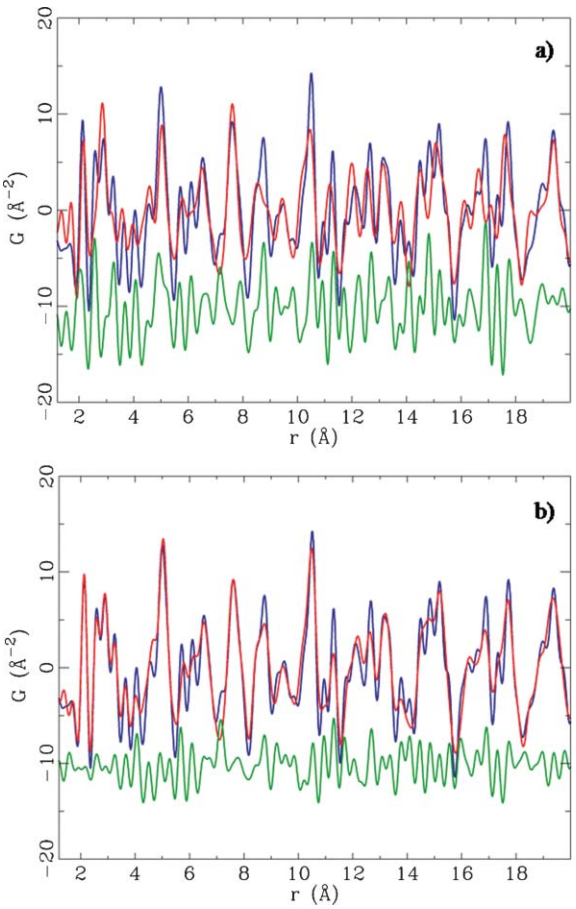

Fig. 7 Reverse Monte Carlo (RMC) results for IE-Li($Ni_{0.5}Mn_{0.5}$)O_2 pristine material: (a) fit before the RMC calculations with the initial random cluster model and (b) after. The blue line represents the experimental data and the red line the calculated PDF. The difference between the calculated and experimental PDFs is shown in green.

Table 4 Number of Ni/Mn pairs in the transition metal layers (ab plane) of IE-Li($Ni_{0.5}Mn_{0.5}$)O_2 and occupational correlation results before and after the RMC calculations, for 12 × 12 × 2 cluster size and for the first and second coordination shells

	$R\bar{3}m$ Space group 12 × 12 × 2 cluster			
	1st Coordination shell		2nd Coordination shell	
	Before (random)	After	Before (random)	After
Ni/Ni pairs (%)	25.0	19.8	24.8	34.5
Ni/Mn pairs (%)	49.5	59.9	50.0	30.6
Mn/Mn pairs (%)	25.5	20.3	25.2	34.9
Total (%)	100	100	100	100
Correlation c_{NiMn}[a]	0.00	−0.20	−0.02	+0.39

[a] The correlation coefficient c_{ij} between a pair of sites i and j is given by the statistical definition[26] of the correlation: $c_{ij} = (P_{ij} - \theta^2)/[\theta(1-\theta)]$, where P_{ij} is the probability that both sites i and j are occupied by the same atom type and θ is its overall occupancy. Negative values of c_{ij} indicate that the sites i and j tend to be occupied by different atom types.

Table 5 Number of cation pairs in the Ni/Mn layers (*ab* plane) of $Na(Ni_{0.5}Mn_{0.5})O_2$ and IE-$Li(Ni_{0.5}Mn_{0.5})O_2$ in the two different ordering schemes (zigzag and chain) and comparison with the RMC calculations for the first and second coordination shells

	Ordering schemes						$Na(Ni_{0.5}Mn_{0.5})O_2$		IE-$Li(Ni_{0.5}Mn_{0.5})O_2$	
	1st Coord. shell			2nd Coord. shell			1st Coord. shell	2nd Coord. shell	1st Coord. shell	2nd Coord. shell
	Random	Zigzag	Chain	Random	Zigzag	Chain	After I; II	After I; II	After I; II	After I; II
Ni/Ni pairs (%)	25	16.7	16.7	25	33.3	16.7	22.5; 19.8	27.1; 26.0	19.8	34.5
Ni/Mn pairs (%)	50	66.7	66.7	50	33.3	66.7	54.2; 56.5	45.1; 44.1	59.9	30.6
Mn/Mn pairs (%)	25	16.7	16.7	25	33.3	16.7	23.3; 23.7	27.8; 29.9	20.3	34.9
Total (%)	100	100	100	100	100	100	100	100	100	100

ordering tendency in the three samples will reflect, at least to some degree, the errors in the PDF method. However, that two different Na samples prepared using different synthetic routes clearly show ordering indicates that the tendency for ordering in this class of materials, as revealed by the RMC calculations, is real. Given the (i) better fit to the data obtained for $Na(Ni_{0.5}Mn_{0.5})O_2$-II and (ii) the lack of absorption problems for this sample, the results for this sample are expected to be the most accurate.

The values for the number of Ni/Ni, Ni/Mn and Mn/Mn pairs for both samples were compared to three possible schemes of Ni/Mn cations arrangements in the layer: chain,[14] zigzag[10] and random. For the first coordination shell (Table 5), the numbers of pairs after the RMC calculations clearly show a non-random distribution of Ni and Mn cations in the TM layers. However, these results do not allow us to distinguish between these two models of ordering. In contrast, those for the second coordination shell (Table 5) clearly show that the structural model obtained after the RMC calculations is consistent with a zigzag arrangement, as previously predicted by Yoon *et al.* by using first principle calculations,[10] in contrast to the flower-like one for SS-$Li(Ni_{0.5}Mn_{0.5})O_2$.[8,12,27] Indeed, in the second coordination shell, the number of Ni/Mn pairs decreases from the random model value (around 50%) to 31% for the IE compound and 44–45% for the Na compound. The values are much closer to the number of Ni/Mn pairs obtained for the zigzag model (33.3%) than to the one obtained for the chain model (66.7%). Thus, both compounds, IE-$Li(Ni_{0.5}Mn_{0.5})O_2$ and its $Na(Ni_{0.5}Mn_{0.5})O_2$ precursor, show a tendency to adopt the zigzag structure, even though, based on the PDF results, this appears to be less pronounced for the Na compound. Given the errors inherent to fitting the PDF data, the true cation arrangement scheme is probably closest to that observed for $Na(Ni_{0.5}Mn_{0.5})O_2$-II.

The zigzag ordering is not perfect, consistent with the lack of superstructure peaks in the diffraction patterns that would be expected for long-range ordering. Note, however, that registry between the ordering in adjacent layers is required for long-range ordering, and the PDF data did not reveal any tendencies for ordering in the third dimension. Analysis of the ^{6}Li NMR lineshape further supports the lack of 3D ordering: the presence of a perfect zig-zag arrangement would result in a limited set of distinct local environments, which should give rise to either well resolved resonances, or a more distinctive lineshape. This is not the case for IE-$Li(Ni_{0.5}Mn_{0.5})O_2$, its broad ^{6}Li NMR lineshape reflecting a wide range of different local environments.

Conclusions

Neutron diffraction data and PDF analysis showed that a perfectly layered structure was obtained for $Na(Ni_{0.5}Mn_{0.5})O_2$ with no Na/Ni disorder. Since ion-exchange is a soft chemical process, this led to well-layered $Li(Ni_{0.5}Mn_{0.5})O_2$ with almost no Li in the transition metal layers, as seen from ^{6}Li MAS NMR experiments. Because of this, the interlayer spacing compared to the SS compound is also larger, likely increasing the Li diffusivity and rate capability, as observed by Kang *et al.* when this material is used as a positive electrode in lithium-ion batteries.[13]

Unlike EXAFS, the PDF technique is sensitive to longer-range correlations, and can give additional information about the local ordering in further coordination shells, which in this case was required to distinguish between different ordering schemes. Ordering of Ni and Mn atoms in the transition metal layers was detected in IE-$Li(Ni_{0.5}Mn_{0.5})O_2$ and the Na precursors: Ni atoms tend to be surrounded by more Mn atoms in the first coordination shell, while an analysis of the second cation coordination shell shows that zigzag ordering of the transition metals is preferred over a chain ordering scheme.

Acknowledgements

The work was supported by the Assistant Secretary for Energy Efficiency and Renewable Energy, Office of FreedomCAR and Vehicle Technologies of the U. S. Department of Energy under Contract No. DE-AC03-76SF00098, *via* subcontracts No. 6517748 and 6517749 with the Lawrence Berkeley National Laboratory. We would also like to acknowledge support from The Electrochemical Society for a Joseph W. Richards Summer Fellowship for J.B., the Center for Materials Science and Engineering (MIT), the MRSEC program of the NSF under award number DMR 02-13282, and the Departament d'Educació i Universitats, de la Generalitat de Catalunya *via* a BP fellowship for J.C. The ISIS Facility of the Rutherford Appleton Laboratory is thanked for access to GEM. This work has benefited from the use of the Intense Pulsed Neutron Source at Argonne National Laboratory. This facility is funded by the U. S. DOE under Contract W-31-109-ENG-38. We are grateful for the assistance given to us at the different beam lines from Winfried Kockelmann (GEM, ISIS), Evan Maxey and Ashfia Huq (GPPD, IPNS). We thank Matthias Gutmann and Alan Soper for their help in neutron data processing, as well as Won-Sub Yoon and Meng Jiang for helpful discussions.

References

1 T. Ohzuku and Y. Makimura, *Chem. Lett.*, 2001, 744.
2 Y. Makimura and T. Ohzuku, *J. Power Sources*, 2003, **119–121**, 156.
3 Z. Lu, D. D. MacNeil and J. R. Dahn, *Electrochem. Solid-State Lett.*, 2001, **4**, A191.
4 K. Mizushima, P. C. Jones, P. J. Wiseman and J. B. Goodenough, *Mater. Res. Bull.*, 1980, **15**, 783.
5 W.-S. Yoon, Y. Paik, X.-Q. Yang, M. Balasubramanian, J. McBreen and C. P. Grey, *Electrochem. Solid-State Lett.*, 2002, **5**, A263.
6 Z. Lu and J. R. Dahn, *J. Electrochem. Soc.*, 2002, **149**, A815.
7 Z. Lu, L. Y. Beaulieu, R. A. Donaberger, C. L. Thomas and J. R. Dahn, *J. Electrochem. Soc.*, 2002, **149**, A778.
8 J. Bréger, N. Dupré, P. J. Chupas, P. L. Lee, T. Proffen, J. B. Parise and C. P. Grey, *J. Am. Chem. Soc.*, 2005, **127**, 7529.
9 S. Meng, G. Ceder, C.P. Grey, W.-S. Yoon and Y. Shao-Horn, *Electrochem. Solid-State Lett.*, 2004, **7**, A155–158.
10 W.-S. Yoon, S. Iannopollo, C. P. Grey, D. Carlier, J. Gorman, J. Reed and G. Ceder, *Electrochem. Solid-State Lett.*, 2004, **7**, A167.
11 Z. Lu, Z. Chen and J. R. Dahn, *Chem. Mater.*, 2003, **15**, 3214.
12 A. Van der Ven and G. Ceder, *Electochem. Commun.*, 2004, **6**, 1045.
13 K. Kang, Y. S. Meng, J. Bréger, C. P. Grey and G. Ceder, *Science*, 2006, **311**, 977.
14 M. S. Islam, R. A. Davies and J. D. Gale, *Chem. Mater.*, 2003, **15**, 4280.
15 A. K. Soper and P. Buchanan, *gudrun*, ISIS Report OX11OQX, Version 1.2, 2001.
16 P. F. Peterson, M. Gutmann, T. Proffen and S. J. L. Billinge, *J. Appl. Crystallogr.*, 2000, **33**, 1192.
17 L.-S. Du, A. Samoson, T. Tuherm and C. P. Grey, *Chem. Mater.*, 2000, **12**, 3611.
18 H. M. Rietveld, *J. Appl. Crystallogr.*, 1969, **2**, 65.
19 A. C. Larson and R. B. Von Dreele, *General Structure Analysis System (GSAS)*, Los Alamos National Laboratory Report LAUR 86–748, Los Alamos National Laboratory, Los Alamos, 2000; B. H. Toby, *J. Appl. Crystallogr.*, 2001, **34**, 210.
20 E. J. Wu, P. D. Tepesch and G. Ceder, *Philos. Mag. B*, 1998, **77**, 1039.
21 J. Brentano and E. O. Hoffmann, *Proc. R. Soc. London, Ser. A*, 1925, **27**, 184.
22 V. F. Sears, *Neutron News*, 1992, **3**, 26.
23 R. L. McGreevy and L. Pusztai, *Mol. Simul.*, 1988, **1**, 359.
24 M. G. Tucker, M. T. Dove and D. A. Keen, *J. Appl. Crystallogr.*, 2001, **34**, 630.
25 T. Proffen and R. B. Neder, *J. Appl. Crystallogr.*, 1997, **30**, 171.
26 T. R. Welberry, *Rep. Prog. Phys.*, 1985, **48**, 1543.
27 Y. Hinuma, Y. S. Meng, K. Kang and G. Ceder, *Chem. Mater.*, 2007, **19**, 1790.